Materials Research. 2016; 19(2): 389-393
DOI:http://dx.doi.org/10.1590/1980-5373-MR-2015-0214

Mechanosynthesis, Crystal Structure and Magnetic Characterization of Neodymium Orthoferrite

Pedro Vera Serna[a]*, Cecilio García Campos[a], Felix Sánchez De Jesús[b], Ana María Bolarín Miró[b], José Antonio Juanico Lorán[c], Jeffrey Longwell[d]

[a]División de Ingenierías, Universidad Politécnica de Tecámac – UPTECAMAC, Tecámac de Felipe Villanueva, Estado de México, Mexico
[b]Área Académica de Ciencias de la Tierra y Materiales, Universidad Autónoma del Estado de Hidalgo – UAEH, Mineral de la Reforma, Hidalgo, Mexico
[c]División de Ingeniería Industrial Nanotecnología, Universidad Politécnica del Valle de México – UPVM, Tultitlan, Estado de México, Mexico
[d]Department of Languages and Linguistics, New Mexico State University – NMSU, Las Cruces, NM USA

Received: April 9, 2015; Revised: November 7, 2015; Accepted: December 23, 2015

Neodymium orthoferrite $NdFeO_3$ was obtained at room temperature by mechanosynthesis with a stoichiometric ratio of Nd_2O_3 and Fe_2O_3 powders, whereas the traditional synthesis requires a temperature of approximately 1000 °C. The crystal structure was analyzed by X-ray diffraction analysis using Cu radiation and a LynxEye XE detector, whose strong fluorescence filtering enabled a high signal intensity. The analysis indicated that the obtained crystallites were nano-sized. The particle morphology was observed by scanning electron microscopy, and the magnetic saturation was tested by vibrating sample magnetometry. The synthesis of $NdFeO_3$ was detected after a few hours of milling, indicating that the milling imparted mechanical energy to the system.

Keywords: *Mechanosynthesis, Ferrites, Neodymium, X-ray diffraction*

1. Introduction

Neodymium-based materials are used in such applications and products as magnetic suspensions [1], photoluminescence [2], measurement of the grain size distribution in thin films [3], magnetic molecules [4], optical ring cores [5], coloring agents for glasses [6], and hard or soft magnets, depending on the crystal structure (a hexagonal or garnet crystal structure for hard magnets and a spinel crystal structure with an applied external magnetic field for temporary, soft magnets). When the external field decreases or disappears, the saturation magnetic value in a soft magnetic material is reduced. In these cases, different material groups exist. Ferrites [7], such as neodymium orthoferrite $NdFeO_3$, are one such group. $NdFeO_3$ is a soft material with an orthorhombically distorted structure derived from a cubic perovskite structure and was recently applied as an anode in solid oxide fuel cells [8,9]. Although there have been various reports of mechanical alloy-based syntheses of $NdFeO_3$, the products were generated under different conditions (generating sub-products) and using different precursors (T. Alonso, Yinong Liu, and P:G:McComirc), such as Ar and Fe_3O_4 [10]. Alternative synthesis methods were studied in 2011 and 2013 [11,12], whereas the ceramic method has been traditionally used for the synthesis of this material. In this report, the mechanosynthesis of $NdFeO_3$ is investigated as an alternative room-temperature method of driving a reaction using impact energy. The energy consumption of this method is markedly lower than that of the traditional synthesis approach, which utilizes temperatures of approximately 1000-1300 °C for periods of 12 or 24 h [10,13,14]. In some cases, the detected nanoscale particles exhibited improved magnetic properties and electric conductivities relative to the microscale particles [15]. The morphology change observed for the materials obtained by mechanosynthesis is possible due to the use of such precursor materials as oxides and carbonates, which allows the reaction to be achieved via oxygen reduction and avoids contamination with acids or toxic gas vapors [16,17]. The process is easy when the precursors are reactive and their atomic diameters and structures are similar.

In this paper, we present the crystal structure, magnetic saturation and particle morphology of $NdFeO_3$ powders obtained by mechanosynthesis using a high-energy shaker/mixer mill at room temperature from Fe_2O_3 and Nd_2O_3 precursors under dry conditions without the use of a noble gas.

2. Experimental

Iron oxide III (Sigma-Aldrich) and neodymium oxide III (Sigma-Aldrich) precursor oxides with a purity of higher than 99% were used in the milling process. The ratio was stoichiometric, as shown in equation 1. The volume of the stainless steel vials was 50 cm^3, and the milling times

*e-mail: pedrovera.upt@gmail.com

tested were 0 h, 1.5 h, 4.5 h, 9 h, 13.5 h and 15 h. The ball-powder mass ratio was 20:1 and the shaker/mixer mill was a Spex 8000 D.

$$1/2\ Fe_2O_3 + 1/2\ Nd_2O_3 \rightarrow NdFeO_3 \quad (1)$$

The crystal structure was evaluated using a Bruker D8 Advance theta-theta X-ray diffractometer (XRD), with 2.2 kW Cu (λ= 0.14051 Å) radiation. The milling product was measured by diffraction in the 5-90° 2θ range with a step size of 0.02º. A LynxEye XE detector was used to provide improved fluorescence filtering and thereby improve the peak intensity. DIFFRAC.TOPAS software, version 4.2, was used for the Rietveld refinement, and the results were then compared with those in the ISCD structural database. The morphology was observed using a JEOL scanning electron microscope at 15 kV, and the magnetic saturation was evaluated using a MicroSense EV7 vibrating sample magnetometer (VSM-EV7) with a maximum field of 18000 Oe.

3. Results and discussion

3.1. Crystal structure characterization

The mixture of Nd_2O_3 and Fe_2O_3 powders was structurally characterized with XRD using the LynxEye XE detector (minimizing fluorescence contamination), which provides easier peak identification relative to traditional devices using Cu radiation. Figure 1 shows the peaks at 0 hours as a baseline. The identified Nd_2O_3 peaks correspond to the ICSD database PDF 00-041-1089 hexagonal structure, those of $Nd_2O_2CO_3$ correspond to PDF 00-037-0806, and those of Fe_2O_3 correspond to the PDF 04-003-2900 cubic structure. Other peaks are also present due to the absorption of hydrogen and oxygen by neodymium as $Nd(OH)_3$, identified in PDF 01-070-0214. The difference in the ionic radii of Fe and Nd is small, allowing the diffusion of Nd in Fe_2O_3, as shown in Figure 2. The synthesized $NdFeO_3$ (PDF 04-010-3990) was detected at 4.5 hours, a similar time to that reported by Alonso et al [10] . Examination of the XRD pattern shows that $Nd(OH)_3$ peaks disappear due to the diffusion of Nd. With additional milling, the structure became orthorhombic, and the maximum quantity of $NdFeO_3$ was synthesized at 13.5 hours, as shown in Figure 3. It is possible to observe only the orthorhombic phase of neodymium ferrite. The hexagonal structure of NdO_3 was transformed to distorted perovskite. The results indicate that the low activation energy allowed the chemical reaction to start at the ambient room temperature within only a few hours, thus minimizing contamination or residual impurities from other materials.

The XRD pattern shown in Figure 4 corresponds to 15 hours of milling; in this pattern, it was possible to identify peaks between 2θ =24º and 2θ =25º, corresponding to Fe_2O_3 (PDF 00-033-0664). This observation was most likely caused by wear and tear on the iron milling balls. Energy dispersive spectrometry (EDS) was used to find possible metallic elements derived from the balls; the results presented in Figure 5 show that iron, oxygen and

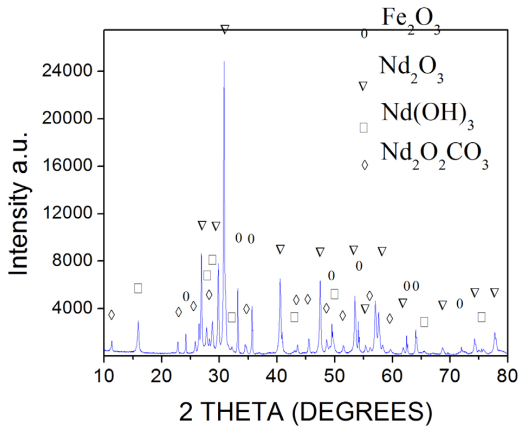

Fig. 1 XRD pattern of the mixture of Nd_2O_3 and Fe_2O_3 with air atmosphere

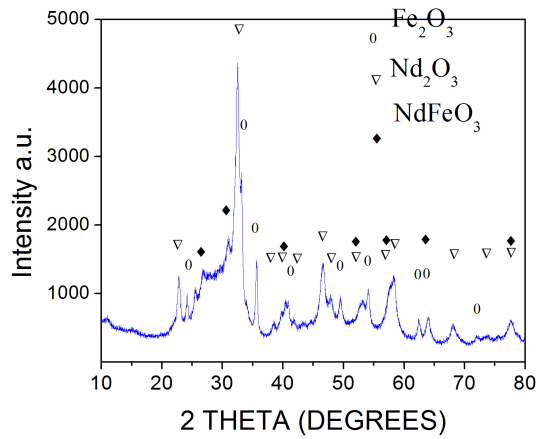

Fig. 2 XRD pattern of powder obtained after 4.5 h of milling from Nd_2O_3 and Fe_2O_3 with air atmosphere.

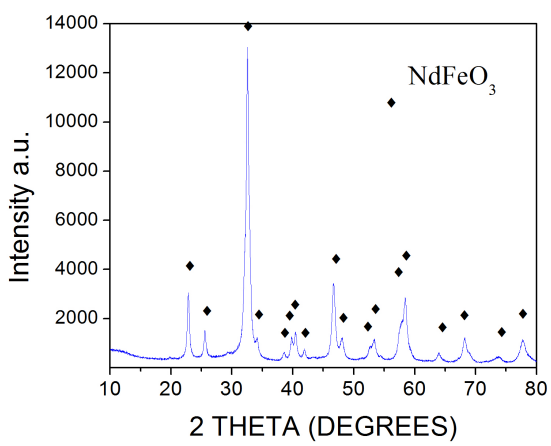

Fig. 3 XRD pattern of powder obtained after 13.5 h of milling from Nd_2O_3 and Fe_2O_3 with air atmosphere

carbon were detected, of which the carbon originated from the polymer used to fix the sample.

The results by weight percent for the powders obtained from the milling process were calculated using Topas software (Figure 6). The optimal mechanosynthesis time for $NdFeO_3$ was 13.5 h. Table 1 shows the weight percentages obtained by Rietveld refinement, and Table 2 shows the lattice parameters.

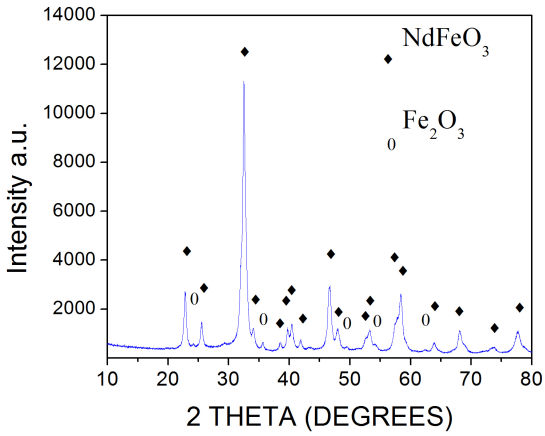

Fig. 4 XRD pattern of powder obtained after 15 h of milling from Nd_2O_3 and Fe_2O_3 with air atmosphere

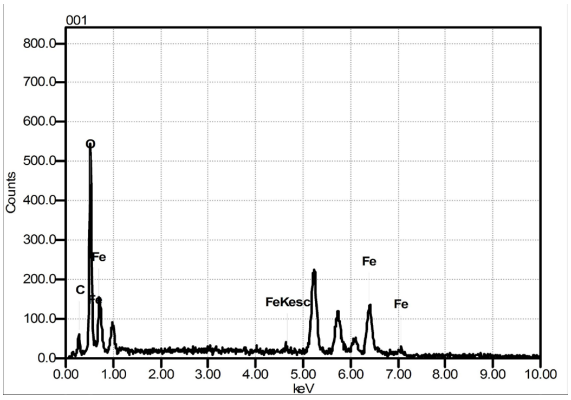

Fig. 5 Iron and carbon detected in SEM after mechanosynthesis of $NdFeO_3$ via 15 h of milling

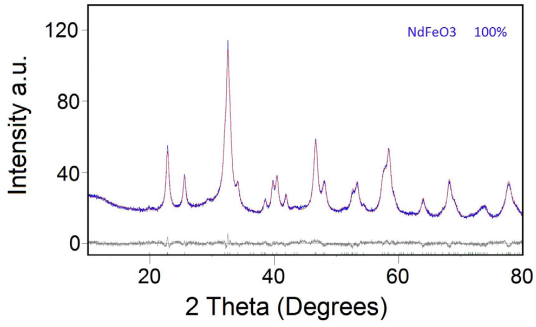

Fig. 6 Phase quantification using Rietveld refinement.

3.2. Particle morphology

Figure 7 shows the particle morphology images. We found that the morphology was irregular during the synthesis process. In the image taken at 0 hours, the particle sizes of the powders are similar, and at 4.5 hours, some particles with dimensions of approximately 10 micrometers were observed. This finding can be attributed to the milling process, in which the particles are deformed and the newly exposed surfaces facilitate the growth of agglomerates and particles. The $NdFeO_3$ phase identified by XRD indicated that the chemical reaction was facilitated by the exposure of new surfaces. As the milling continued, different particle sizes were detected at 4.5 hours, while the particles observed at 9 hours had similar morphologies. Finally, 13.5 hours, the particles were small with a narrow size distribution.

The images presented in Figure 8 suggest that the $NdFeO_3$ particles obtained after 13.5 hours of milling were smaller than those obtained using the mixture of Nd_2O_3 and Fe_2O_3, as the particles in the center of the right-hand image are smaller than those in the left-hand image. The increased interaction between the reactants due to the milling process and the exposure of new surfaces favored the chemical reaction.

3.3. Magnetic saturation characterization

The magnetic saturation data for powders obtained at different milling times are shown in Figure 9. It is well known that mechanosynthesis changes the crystal structure of materials, thereby modifying their magnetic behavior. The magnetic saturation for $NdFeO_3$ obtained herein (1.15 emu/g) was superior to the value obtained by Hu et al. (0.8 emu/g) and similar to the value reported for $NdFeO_3$ with cubic morphology by Wang et al. [18,19]. At 15 hours of milling, corresponding to the time at which carbon was detected, the magnetic saturation was inferior to that obtained after 13.5 hours of milling. Interestingly, when the phase transformation began (4.5 hours), the magnetic saturation was 1.54 emu/g, superior to the values reported for other ferrites.

Table 1 Powder composition as weight percent

Milling time	$NdFeO_3$ (Weight %)	Fe_2O_3 (Weight %)	Nd_2O_3 (Weight %)
4.5 h	54.84	35.85	9.31
9 h	82.89	17.11	-
13.5 h	100%	-	-

Table 2 Lattice parameter values and crystallite size

Phase	a (Å)	b (Å)	c (Å)	Crystallite Size (nm)
$NdFeO_3$	5.5791	7.7637	5.4430	36.5

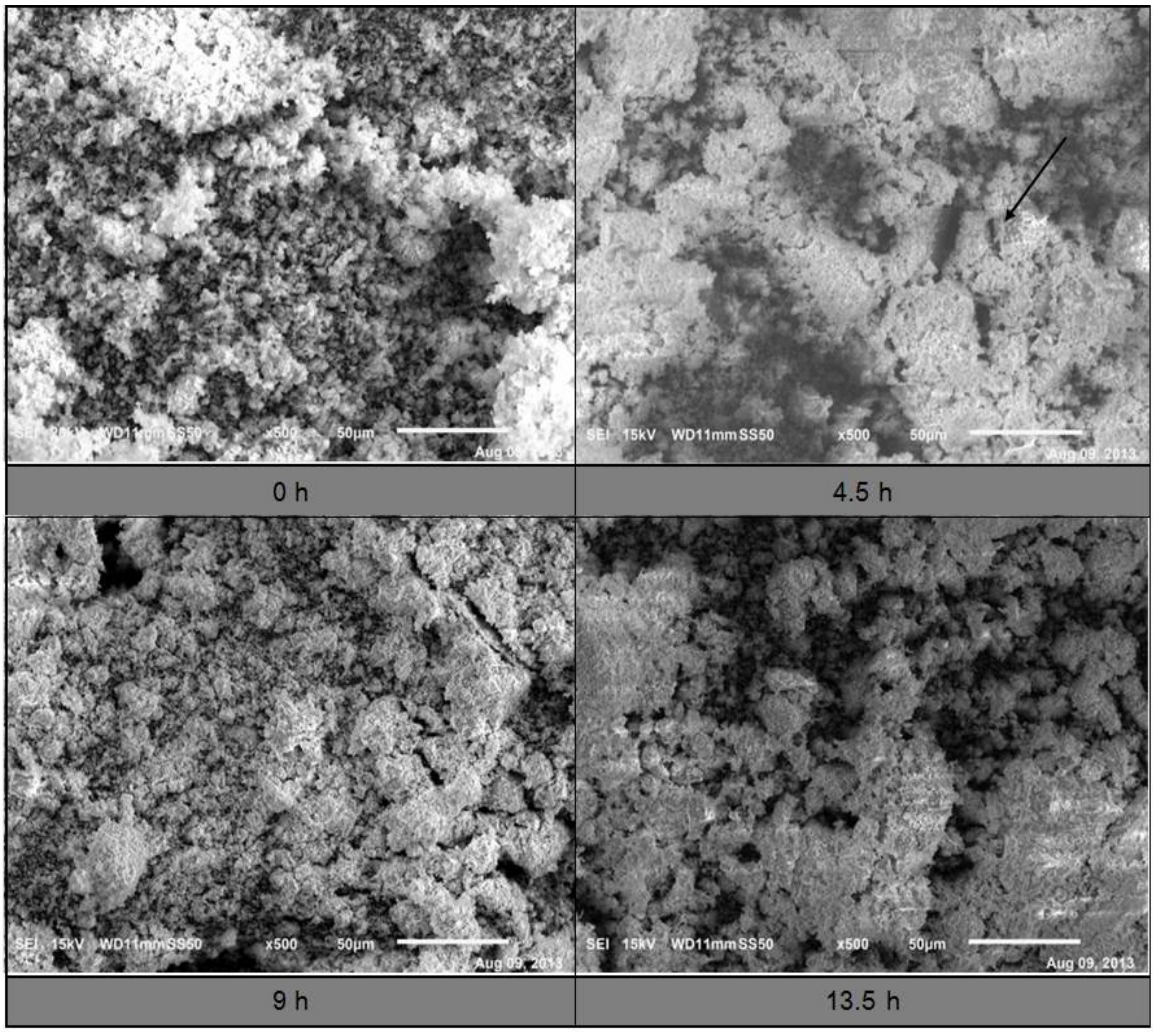

Fig. 7 SEM images of Nd_2O_3-Fe_2O_3 after 0, 4.5, 9 and 13.5 hours of milling.

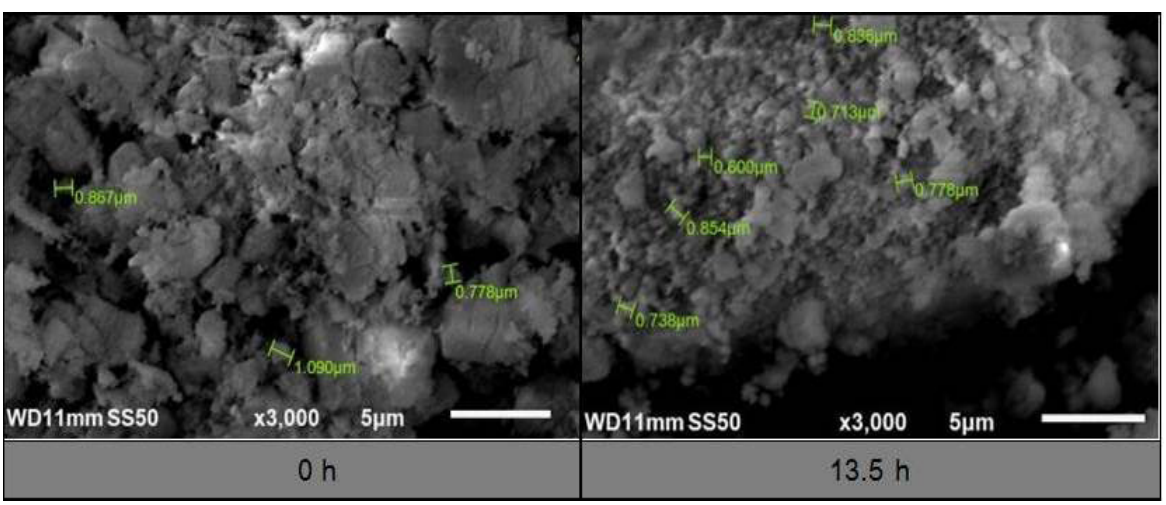

Fig. 8 SEM images of Nd_2O_3-Fe_2O_3 after 0 and 13.5 h of milling

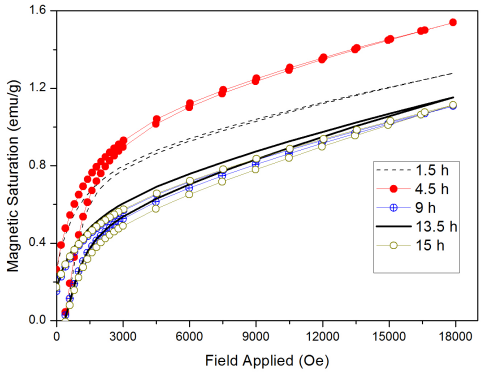

Fig. 9. Hysteresis loops at H_{max}=18 kOe measured at room temperature for oxide powders milled from (Nd_2O_3+ Fe_2O_3)

4. Conclusion

The mechanosynthesis of $NdFeO_3$ from the stoichiometric ratio of Nd_2O_3 and Fe_2O_3 powders was possible at room temperature, avoiding the high temperature (1000 °C) required when using the calcination method. The synthesis yield was close to 100% at 13.5 hours of milling, and the $NdFeO_3$ phase was detected after 4.5 hours of milling, as indicated by the formation of new surfaces after a few hours. The mechanosynthesis modified the crystal structure, reduced the particle size and increased the magnetic saturation above that of other orthoferrites. Our report provides new information about the morphology and magnetic saturation of this material and unprecedentedly high-resolution XRD results obtained using a LynxEye XE detector with Cu radiation.

References

1. Omijeh BO, Nmom CS, Nlewem E. Modeling of a vertical axis wind turbine with permanent magnet synchronous generator for Nigeria. *International Journal of Engineering and Technology*. 2013; 3 (2): 212-220. http://iet-journals.org/archive/2013/feb_vol_3_no_2/9183451357665481.pdf
2. Pashayev AM, Tagiyev BG, Abushov SA, Tagiyev OB, Kazimova FA. Photoluminescence of $EuGa_2Se_4$:Nd^{3+}. *Optics and Photonics Journal*. 2012;2(1):59-60. http://dx.doi.org/10.4236/opj.2012.21009
3. Zielinski M, Wojcieszak D, Domaradzki J, Kaczmarek D, Prociow E. Influence of neodymium dopant on TiO2 structure. *Electronics Technology (ISSE) IEEE Explore*. 2010; doi: 10.1109/ISSE.2010.554725
4. Fahrendorf S, Atodiresei N, Besson C, Caciuc V, Mathes F, Blugel S, et al. Accessing 4f-states in single-molecule spintronics. *Nature Communications*. 2012;4(2425): 1-6. doi:10.238/ncomms3425.
5. Dorosz D. Ring-core optical fibre doped with neodymium. In: *SPIE 6347, Photonics Applications in Astronomy, Communications, Industry, and High-Energy Physics Experiments. Proceedings*. Wilga, Poland: 2006. doi:10.1117/12.714636.
6. Guo X, Li X, Yang H, Zhao J, Zhao W. Effect of neodymium on the crystallization, microstructure and colorization of Li_2O-Al_2O_3-SiO_2. *New Journal of Glass and Ceramics*. 2012;2:98-103. doi:10.4236/njgc.2012.22014.
7. Özgür U, Alivov Y, Morkoç H. Microwave Ferrites. Part 1: Fundamental properties. *Journal of Materials Science: Materials in Electronics*. 2009;20(2):789-807.
8. Ahmad I, Akhtar MJ, Younas M, Siddique M, Hasan MM. Small polaronic hole hopping mechanism and Maxwell-Wagner relaxation in $NdFeO_3$. *Journal of Applied Physics*. 2012;112(7):074105. doi: 10.1063/1.4754866
9. Chen T, Sheng L, Liu F, Zhu W, Zhang Q, Chu X. NdFeO3 as node material for S/O2 solid oxide fuel cells. *Journal of Rare Earths*. 2012;30(11):1138-1141. doi:10.1016/S1002-0721(12)60194-X
10. Alonso T, Liu Y, McCormick PG. Synthesis of $NdFeO_3$ by mechanical alloying. *Journal of Materials Science Letters*. 1992;1(3):164-166.
11. Hao YJ, Li B, Liu RH, Li FT. Synthesis of NdFeO3 Perovskites in a reverse microemulsion and its visible light photocatalytic activity. *Advanced Material Research*. 2011;282-283:593-596. doi:10.4028/www.scientific.net/AMR.282-283.593
12. Singh S, Singh A, Yadav BC, Dwivedi PB. Fabrication of nanobeads structured perovskite type neodymium iron oxide film: its structural, optical, electrical and LPG sensing investigations. *Sensors & Actuactors: B. Chemical*. 2013;177: 730-739. doi:10.1016/j.snb.2012.11.096
13. Wen Q, Xu Y, Xu B, Fasel C, Guillon O, Buntkowsky G, et al. Single-source-precursor synthesis of dense SiC/HfC(x)N(1-x)-based ultrahigh-temperature ceramic nanocomposites. *Nanoscale*. 2014;6(22):13678-89. doi: 10.1039/c4nr03376k.
14. Wang Y, Cao S, Shao M, Yuan S, Kang B, Zhang J, et al. Growth rate dependence of the NdFeO3 single crystal grown by float-zone-technique. *Journal of Crystal Growth*. 2010;318:927–931.
15. Yoo JW. Toward improved selectivity of targeted delivery: The potential of magnetic nanoparticles. *Archives of Pharmaceutical Research*. 2012;35(1):1-2. doi: 10.1007/s12272-012-0100-4.
16. Strukil V, Igrc MD, Eckert-Maksic M, Friscic T. Click mechanochemistry: quantitative synthesis of "ready to use chiral organocatalysts by efficient two-fold thiourea coupling to vicinal diamines. *Chemistry*. 2012;18 (27):8464-8473, doi: 10.1002/chem.201200632
17. Di Leo P, Pizzigallo MD, Ancona V, Di Benedetto F, Mesto E, Schingaro E, et al. Mechanochemical degradation of pentachlorophenol onto birnessite. *Journal of Hazardous Materials*. 2012;244-245:303-310. doi:10.1016/j.jhazmat.2012.11.037.
18. Hu GH, Umehara I, Shuang X, Yuan S, Cao SX. Pressure effect in multiferroic phase transition of perovskite ferrite crystals NdFeO3 and ErFeO3. *Journal of Physics: Conference Series*. 2012;400(Pt 3): 032023. doi: 10.1088/1742-6596/400/3/032023
19. Wang Y, Yan X, Chen J, Deng J, Yua R, Xing X. Shape controllable synthesis of NdFeO3 micro single crystals by a hydrothermal route. *CrystEngComm*. 2014;16:858-852. doi: 10.1039/C3CE41434E